



# Visual interpretation of [<sup>18</sup>F]Florbetaben PET supported by deep learning–based estimation of amyloid burden

Ji-Young Kim<sup>1,2</sup> · Dongkyu Oh<sup>1</sup> · Kiyoung Sung<sup>3</sup> · Hongyoon Choi<sup>1</sup> · Jin Chul Paeng<sup>1</sup> · Gi Jeong Cheon<sup>1,4,5</sup> · Keon Wook Kang<sup>1</sup> · Dong Young Lee<sup>3,6</sup> · Dong Soo Lee<sup>1,7</sup>

Received: 27 May 2020 / Accepted: 15 September 2020  
© Springer-Verlag GmbH Germany, part of Springer Nature 2020

## Abstract

**Purpose** Amyloid PET which has been widely used for noninvasive assessment of cortical amyloid burden is visually interpreted in the clinical setting. As a fast and easy-to-use visual interpretation support system, we analyze whether the deep learning–based end-to-end estimation of amyloid burden improves inter-reader agreement as well as the confidence of the visual reading.

**Methods** A total of 121 clinical routines [<sup>18</sup>F]Florbetaben PET images were collected for the randomized blind-reader study. The amyloid PET images were visually interpreted by three experts independently blind to other information. The readers qualitatively interpreted images without quantification at the first reading session. After more than 2-week interval, the readers additionally interpreted images with the quantification results provided by the deep learning system. The qualitative assessment was based on a 3-point BAPL score (1: no amyloid load, 2: minor amyloid load, and 3: significant amyloid load). The confidence score for each session was evaluated by a 3-point score (0: ambiguous, 1: probably, and 2: definite to decide).

**Results** Inter-reader agreements for the visual reading based on a 3-point scale (BAPL score) calculated by Fleiss kappa coefficients were 0.46 and 0.76 for the visual reading without and with the deep learning system, respectively. For the two reading sessions, the confidence score of visual reading was improved at the visual reading session with the output ( $1.27 \pm 0.078$  for visual reading-only session vs.  $1.66 \pm 0.63$  for a visual reading session with the deep learning system).

**Conclusion** Our results highlight the impact of deep learning–based one-step amyloid burden estimation system on inter-reader agreement and confidence of reading when applied to clinical routine amyloid PET reading.

**Keywords** Alzheimer’s disease · Amyloid PET · [<sup>18</sup>F]Florbetaben · PET · Visual quantification · Deep learning

---

This article is part of the Topical Collection on Neurology

**Electronic supplementary material** The online version of this article (<https://doi.org/10.1007/s00259-020-05044-x>) contains supplementary material, which is available to authorized users.

---

✉ Hongyoon Choi  
chy1000@snu.ac.kr

<sup>1</sup> Department of Nuclear Medicine, Seoul National University Hospital, Seoul, Republic of Korea

<sup>2</sup> Department of Nuclear Medicine, Seoul National University Bundang Hospital, Seongnam, Republic of Korea

<sup>3</sup> Department of Neuropsychiatry, Seoul National University Hospital, Seoul, Republic of Korea

<sup>4</sup> Institute on Aging, Seoul National University, Seoul, Republic of Korea

<sup>5</sup> Radiation Medicine Institute, Seoul National University College of Medicine, Seoul, Republic of Korea

<sup>6</sup> Department of Psychiatry, Seoul National University College of Medicine, Seoul, Republic of Korea

<sup>7</sup> Department of Molecular Medicine and Biopharmaceutical Sciences, Graduate School of Convergence Science and Technology, Seoul National University, Seoul, Republic of Korea

## Introduction

Alzheimer's disease is the most main cause of dementia worldwide [1]. Both clinical signs and histopathological confirmation by brain biopsy or autopsy were needed for a definitive diagnosis of Alzheimer's disease [2–5]. The amyloid burden estimated by positron emission tomography (PET) is highly correlated with the presence and density of amyloid loading at autopsy [6]. Therefore, amyloid PET plays a critical role in the diagnosis and predicting prognosis of Alzheimer's disease as well as mild cognitive impairment (MCI) [4]. Despite the importance of the objective and accurate amyloid PET interpretation, the analysis is mostly based on the degree of an amyloid burden by qualitative visual reading [4].

The gold standard of the interpretation of amyloid PET, particularly recent amyloid PET imaging based on F-18- labeled radiotracers, is the visual reading performed by experts, which has intrinsic limitations in inter-reader variability and objectiveness [7]. A few studies have demonstrated improvement of qualitative interpretation of amyloid PET when readers interpreted with quantification results [8, 9]. Although the quantification results could reduce inter-reader variability in visual scoring, quantification of amyloid PET is poorly used in the clinical setting due to usage limitations of the quantification tools that often require additional time and effort in busy routine clinical settings. One critical restraint is that structural MRI is often required for many quantification methods to define volume-of-interests and generate spatially normalized amyloid PET [10, 11]. Although some recent tools can also provide quantification of amyloid PET data without structural MRI, many still depend on preprocessing steps, such as spatial warping and selecting template [10–13], limiting routine clinical use. Recent advances in deep learning providing new methods to estimate amyloid PET patterns using machine learning–based algorithms without manual processing image features have been developed [14, 15]. In this regard, we developed a fast and easy-to-use automated one-step estimation of amyloid burden application based on deep learning via end-to-end training [14], considering that a deep learning–based system that uses a native-space amyloid PET without preprocessing could support a visual effectively reading in a busy clinical environment.

In the study, we applied the one-step amyloid estimation system based on deep learning to the visual reading of amyloid PET images as routine clinical practice. We analyzed the inter-reader agreement and confidence evaluated by the visual interpretation-only and the visual interpretation with the deep learning system to show the improvement of interpreting amyloid PET.

## Methods

### Subjects

We recruited 121 [<sup>18</sup>F]Florbetaben PET data (M: 36, F: 85; mean age  $\pm$  SD: 74.31  $\pm$  7.28) retrospectively who visited the memory clinic of the Seoul National University Hospital and underwent [<sup>18</sup>F]Florbetaben PET from Jan 2019 to May 2019. The subjects included 29 patients with dementia (21 Alzheimer's disease (AD), 3 vascular dementia (VD), 2 dementia with lewy bodies (DLB), 1 frontotemporal dementia (FTD), and 2 dementia not otherwise specified), 68 patients with mild cognitive impairment (MCI: 60 amnesic and 8 non-amnesic MCI), and 24 subjective cognitive impairment (SCI). A diagnosis of dementia was made according to the criteria of the fourth edition of the Diagnostic and Statistical Manual of Mental Disorders [16]. AD was diagnosed according to the probable or possible AD criteria of the National Institute of Neurological and Communication Disorders and Stroke/AD and Related Disorders Association (NINCDSADRDA) [17]. VD was diagnosed according to the probable or possible VD criteria of the National Institute of Neurological Disorders and Stroke-Association Internationale pour la Recherche et l'Enseignement en Neurosciences (NINDS-AIREN) [18]. DLB was diagnosed according to the DLB consensus criteria [19] and frontotemporal dementia (FTD) was diagnosed according to the FTD consensus criteria [20]. MCI was diagnosed according to current consensus criteria [21]. SCI was defined as the presence of a cognitive impairment with presentation at a memory clinic but normal cognition on tests [22].

No subjects were excluded to simulate a usual clinical reading environment. The retrospective study was formally approved by the institutional review boards (SNUH IRB Registration Number 2004-047-1116) at our center, and informed consent was withdrawn due to the retrospective design. The study was conducted according to the ethical standards and the 1964 Helsinki declaration.

### [<sup>18</sup>F]Florbetaben PET images

All patients underwent a 20 min positron emission scan at 90 min after the bolus intravenous injection of [<sup>18</sup>F]Florbetaben 296 MBq (8 mCi) using dedicated PET/CT scanners (Biograph mCT40 or mCT64, Siemens Healthcare, Germany). CT scan was used for attenuation correction, followed by an emission scan of the brain. PET images were reconstructed on 400  $\times$  400 image size with a 1  $\times$  1  $\times$  1.5 mm voxel size. Images were reconstructed with ordered subset expectation maximization with 24 subsets and 6 iteration numbers. Post-reconstruction Gaussian filter (full width at half maximum 2 mm) was applied.

### Visual reading of amyloid PET

The effect of the one-step quantification estimation using a deep learning system on visual reading was assessed. The overall design of this study is represented in Fig. 1. Three expert readers performed visual interpretation for 121 [<sup>18</sup>F]Florbetaben PET images. Three readers performed the visual reading consisted of two sessions, interpretation with or without the estimated score of amyloid burden provided by the deep learning system. Three readers qualitatively interpreted brain amyloid plaque loading based on the Brain Amyloid Plaque Load (BAPL) score (1: no amyloid load, 2: minor amyloid load, and 3: significant amyloid load) and the confidence score on a 3-point scale (0: ambiguous, 1: probably, and 2: definite to decide) [23]. The visual interpretation was based on the guideline of [<sup>18</sup>F]Florbetaben PET [23]. All three readers were trained for the visual reading of amyloid PET according to the guidelines and had experience on amyloid PET reading as a clinical routine (9-year, 5-year, and 3-year experienced for amyloid PET reading, respectively). Briefly, typical transverse amyloid PET slices at different brain levels including frontal, cingulate, parietal, temporal, and cerebellar cortices of an individual judged as a visual BAPL score [23]. Furthermore, amyloid PET scans were classified into two groups, negative and positive scans: 1 BAPL scores = negative scans, 2 and 3 BAPL scores = positive scans [23].

The estimation of amyloid burden using the deep learning system was obtained by directly entering reconstructed Dicom images of [<sup>18</sup>F]Florbetaben PET. The deep learning system provided an estimated standardized-uptake-value ratio (SUVR) for frontal, cingulate, parietal, and temporal cortices as the reference to the whole cerebellar region. Thus, quantitative information was predicted by the one-step estimation model based on end-to-end training of the deep learning model. This model was trained by multicenter native-space PET images from the Alzheimer’s Disease Neuroimaging Initiative, which included images acquired by variable hardware and reconstruction algorithms [14, 24]. Detailed architectures and the training process of the model were described in the previous report [14]. The readers interpreted a visual reading-only at the first reading session, and then the readers re-evaluated amyloid PET again assisted by the quantification estimation results provided by the deep learning system. At the second reading session, the readers re-evaluated the BAPL scale again referring the estimated SUVR provided by the deep learning model. Notably, the specific cut-off of SUVR was not used but overall distribution data of the estimated SUVR of population were reviewed before the reading to refer individual SUVR for visual analysis. The two reading sessions had at least 2-week interval.

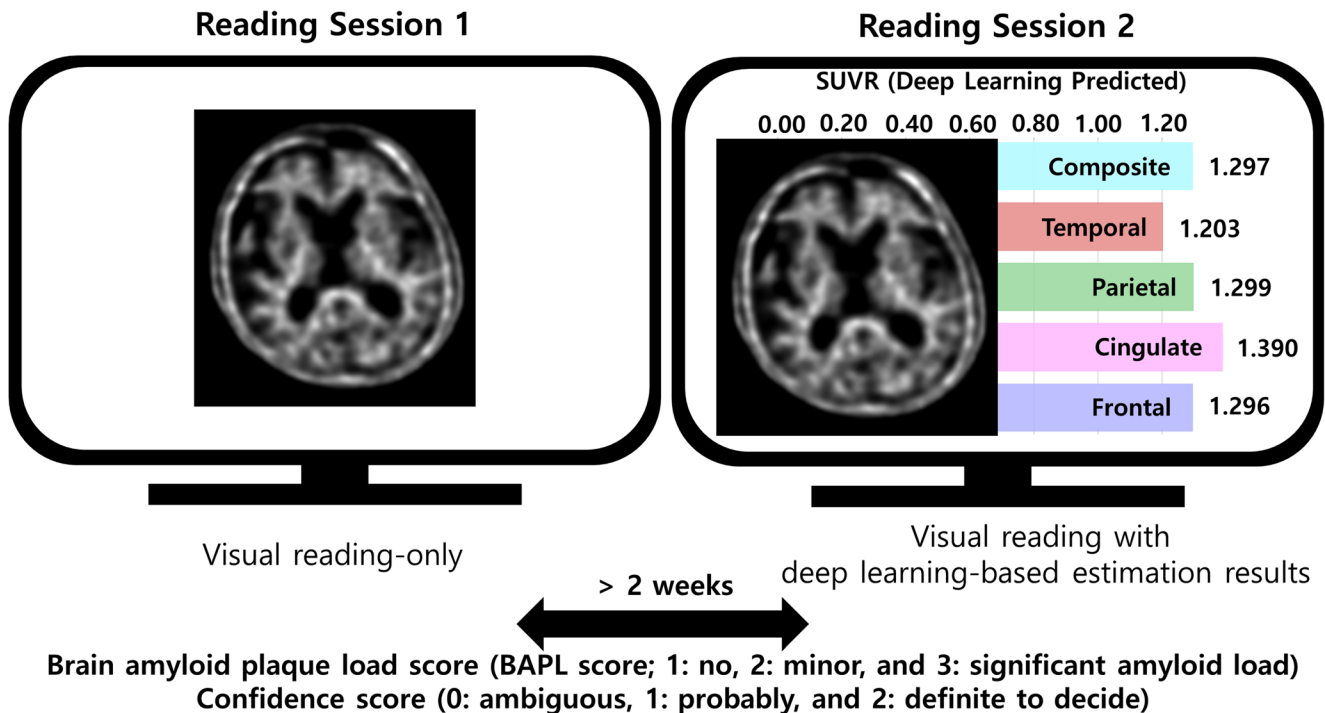


**Fig. 1** The overall workflow of this study. The visual reading with separated two reading sessions with or without a deep learning-based amyloid burden estimation system was performed. The three readers visually interpreted amyloid burden based on the brain amyloid plaque load

(BAPL) score and the confidence score on a 3-point scale (from 0—obscure to 2—easy to decide) at each reading session. In two reading sessions at least 2 weeks apart. Inter-reader variability and confidence score were evaluated

## Statistical analysis

The inter-reader reliabilities were measured by Fleiss kappa coefficients in interpersonal variability and confidence score, respectively. A paired *t* test was applied to assess the difference in confidence scores and a *p* value of < 0.05 was considered statistically significant. The statistic computing was measured using Python (version 3.6.9) and Scipy package (version 1.4.1).

## Results

We performed the randomized blind-reader study using [<sup>18</sup>F]Florbetaben PET images clinically routinely obtained. Three readers have 9-years' 5-years', and 3-years' experience for general and amyloid PET reading, respectively. The BAPL score was reevaluated for each reader after a minimum of 2 weeks as a second reading session with the deep learning-based amyloid estimation system (Fig. 1). The inter-reader agreement of visual reading amyloid PET quantification with or without deep learning results is shown in Table 1. The cross-tables for the readers according to different reading sessions are summarized in Supplementary Table 1. The Fleiss kappa coefficients (95% confidence interval (CI)) of the inter-reader agreement for the classification for a 3-point scale of BAPL scores were 0.47 (95% CI: 0.39–0.59) and 0.76 (95% CI: 0.71–0.85) for the visual reading only and with the deep learning-based estimation, respectively. When PET images were divided into two classes, amyloid-positive and negative, inter-reader agreements were 0.62 and 0.85 for the two reading sessions, respectively.

We also assessed the impact of the deep learning-based system on the confidence of visual interpretation. The confidence score of visual reading was significantly increased at the visual reading session with the deep learning system ( $1.27 \pm 0.78$  for visual reading only and  $1.66 \pm 0.62$  for visual reading with the deep learning

system;  $t = -9.62$ ,  $p < 0.001$ ) (Fig. 2a). On a 3-point scale, the total number of 0-point, low confidence in visual reading, was 74 (20.39%) at the visual reading-only session, which was reduced to 29 (7.99%) at the reading session with the deep learning system. Additionally, the total number of 2-point, high confidence in visual reading, was increased, from 171 (47.11%) to 267 (73.55%) (Fig. 2b). All three readers showed increased confidence score, though the level of experience in amyloid PET was different (Supplementary Fig. 1). Waterfall plots represented the estimated SUVR of amyloid PET with the inter-reader agreement (Fig. 3a, b) and the confidence score (Fig. 3c, d). Among 121 amyloid PET images, 52.1% of images were agreed for all readers at the visual reading-only session, while 78.5% of images were agreed for all readers at the visual reading with the deep learning system. Among PET images that show estimated SUVR ranged from 1.1 to 1.4, 28.6% images were agreed for all readers based on BAPL score on a 3-point scale at the visual reading-only session. However, 63.3% of these images were agreed for all readers at the visual reading session with the deep learning system. The confidence score was also increased after the use of the deep learning-based system (Fig. 3c, d). Of note, a relatively low confidence score at the reading session with the deep learning-based system was found in PET images with SUVR ranged from 1.1 to 1.4, which suggested equivocal cases of amyloid PET [25].

## Discussion

The visual reading of amyloid PET is used to evaluate brain amyloid positivity in routine clinical practice as it is regarded as a gold standard for non-invasive assessment of cortical amyloid burden [23, 26]. Nevertheless, the limitation in objectiveness and inter-reader variability is inevitable. Thus, amyloid PET with equivocal amyloid deposits has been a problem in the diagnosis of dementia [27, 28]. To reduce this

**Table 1** The visual reading of amyloid PET quantification with or without deep learning-based amyloid estimation results

	The first reading session Visual interpretation-only	The second reading session Visual interpretation with deep learning-based amyloid estimation
Fleiss kappa coefficient for BAPL score (3-point scale)	0.465	0.759
Fleiss kappa coefficient for negative/positive PET scan (2-point scale)	0.621	0.852
Confidence score (mean $\pm$ SD)	$1.27 \pm 0.78$	$1.66 \pm 0.62$
Confidence score	0-point (ambiguously)	29
	1-point (probably)	67
	2-point (definitely)	267

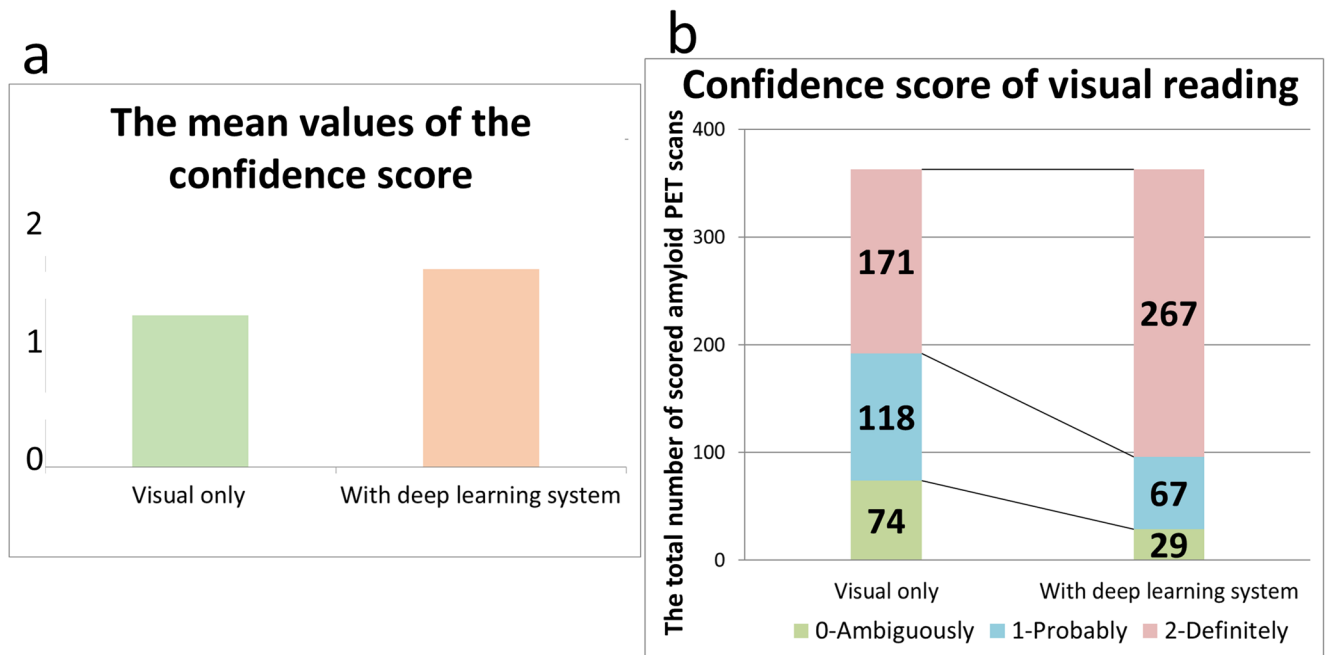


**Fig. 2** The differences in confidence score supported by the deep learning-based system. **a** The confidence score of visual interpretation with the deep learning-based system was significantly higher than those of visual interpretation only ( $1.27 \pm 0.78$  for visual reading only and  $1.66$

$\pm 0.62$  for visual reading with the deep learning system;  $t = -9.62$ ,  $p < 0.001$ ). **b** The distribution of scores was changed according to the usage of the deep learning-based system

ambiguity and increase the inter-reader agreement, the use of quantification of amyloid PET in the clinical routine practice has been attempted [6, 14, 24]. Conventional amyloid PET quantification requires multiple and complicated steps that limit to be utilized in routine clinical use. For example, most quantification methods require structural MRI combined with amyloid PET to identify gray matter and spatially normalize to the template space. However, because of the high cost, both PET and MRI are not always obtained. Furthermore, complicated steps of preprocessing, which are even more not standardized, limit the usage of quantification supporting visual interpretation in the clinical routine. Therefore, the estimation of amyloid PET has depended on visual interpretation-only in many centers even though quantification methods could enhance the reading improvement [8, 9].

The main advantage of our assessment is the improvement of visual reading in terms of the inter-reader agreement and confidence. Our findings are consistent with recent studies that showed increased inter-reader agreement in amyloid PET interpretation by quantitative information [8, 9]. The SUVR values were used for categorizing amyloid images that help to increase inter-reader agreement [29]. The increased inter-reader agreement by using quantification or objective stratification may help early detection of cerebral amyloid load in clinical practice [15, 30]. Compared with other previous works, the estimation of amyloid PET quantification was obtained by the one-step process, which only required native-

space PET images with reconstructed Dicom-formatted files [14, 24].

We could obtain the estimation results to support visual interpretation with a simple process. Practically, we used a web-based application to embed this system run on a server computer, and each client connected to obtain the estimation results of amyloid burden (Supplementary Fig. 2). Notably, SUVR ranged from 1.1 to 1.3 was considered as a borderline of amyloid positivity according to the overall results; thus, the borderline range was visualized on the web-based application. Since the total estimation time was less than 5 s, the estimation result could be easily referred to during visual reading to make more confident visual grading of amyloid PET.

Our results showed increases in inter-reader agreement and confidence in visual reading sessions with the deep learning system. Moreover, the inter-reader agreement was increased in PET images with equivocal amyloid positivity. Despite the use of the deep learning-based system, PET images with equivocal amyloid positivity remained to show relatively low confidence score compared with other amyloid PET images. We represented a few cases with low confidence scores in both sessions with disagreement in visual reading (Supplementary Fig. 3). Notably, these equivocal cases were not improved by the deep learning-based estimation in terms of confidence score, because of borderline quantification results. Nonetheless, a visual reading supported by the deep learning system may improve the communication between



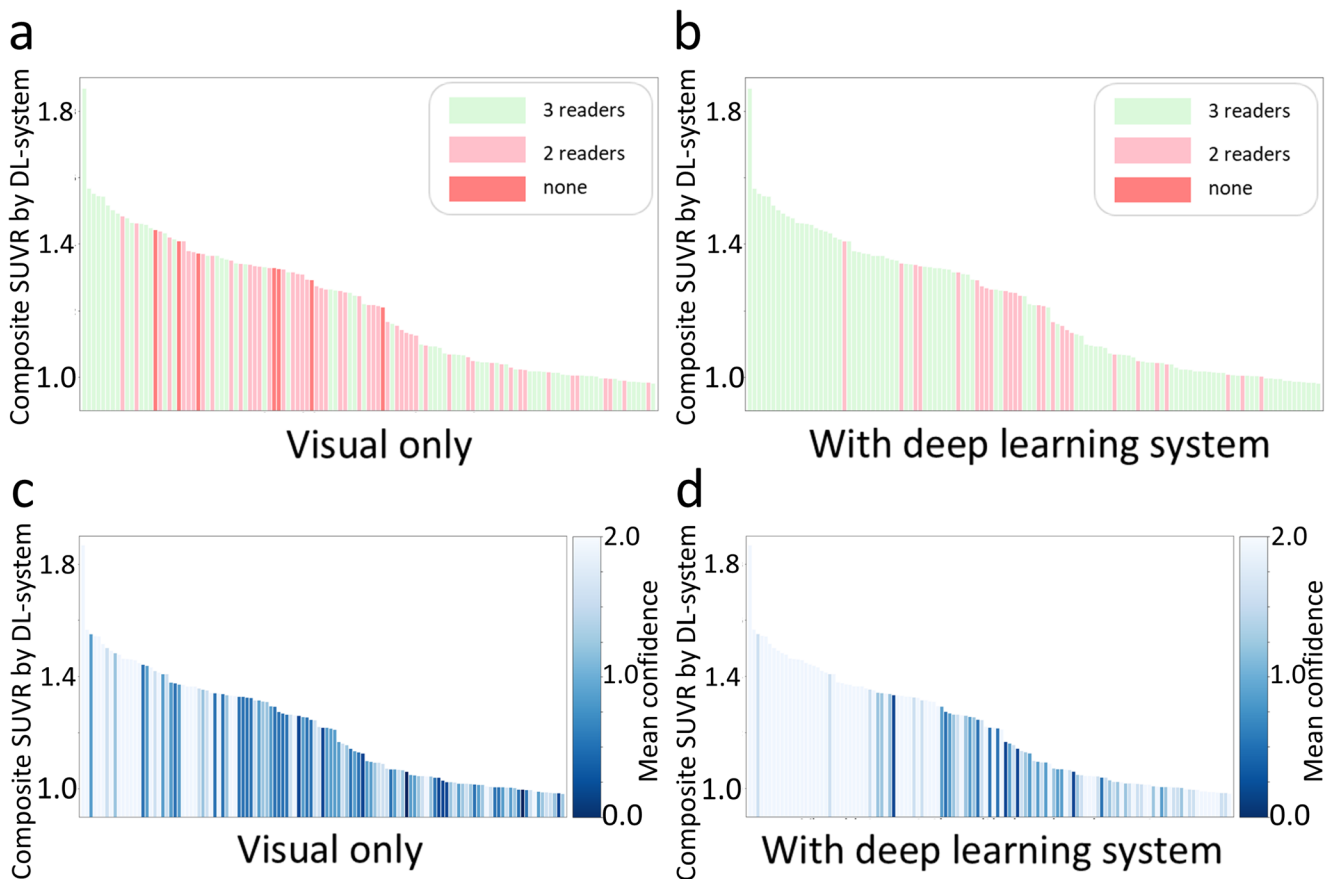


**Fig. 3** The inter-reader agreement and confidence score according to deep learning-based amyloid estimation results. The estimated results of the amyloid burden by deep learning were represented with the inter-reader agreement in 121 amyloid PET scans among 3 readers for the visual interpretation-only session (a) and visual interpretation with the deep learning-based estimation results (b). The estimated results were also represented with the confidence score for the visual interpretation-

only session (c) and visual interpretation with the deep learning-based estimation results (d). The color indicates the agreement of the number of the same results among 3 readers (green: the same amyloid quantification among 3 readers, pink: the same amyloid quantification of 2 readers, and red: difference amyloid quantification among 3 readers (a, b). The colormap indicates the mean of confidence scores among 3 readers (c, d)

reading experts and clinicians as the reading was supported by an objective estimation result. As future work, the role of estimation of amyloid burden using the deep learning system in the clinical decision making beyond visual amyloid positivity should be further validated.

Even though the deep learning system helps visual reading of amyloid PET in reducing subjectivity and ambiguity, there is still a limitation in this study. This study is limited by its retrospective nature, conducted in a single-center, and used only [ $^{18}\text{F}$ ]Florbetaben radiotracer. The standard Centiloid quantification was developed to harmonize multiple tracers and multicenter of amyloid PET that critical to sustain the reliable decision of each tracer [31]. We need to validate its usefulness in the clinical practice by multiple tracers and a multicenter prospective study using native-space amyloid PET data with various scanners. The inclusion of a large scale of native-space amyloid images with multiple tracers, various scanners, and different reconstruction methods could have a great impact on clinical practice that would reflect the worth of

the reading support system. Another limitation is that the subject information of characteristics such as age, sex, clinical diagnosis, and cortical atrophy status was ignored when the reader interpreted visual amyloid PET quantification. The amyloid PET scans in this study were performed as a baseline evaluation and it was not sufficient to include clinical follow-up to assess the impact of the deep learning-based estimation on final diagnosis. Furthermore, the formal reports of [ $^{18}\text{F}$ ]Florbetaben PET made by the consensus of visual reading of multiple readers were used for the clinical diagnosis; thus, it was hard to evaluate whether the model could change clinical diagnosis. As further work, a prospective study to evaluate the impact of deep learning-based estimation on the diagnosis determined by long-term follow-up and the clinical course can be investigated. Besides, we used the estimated amyloid burden by deep learning method which was not directly calculated by conventional image processing including image co-registration, segmentation, and normalization [14, 32–35]. Therefore, the use of estimation results without any

visual reading might be dangerous particularly for the PET scans with equivocal amyloid positivity as well as abnormal space-occupying brain lesions that affect amyloid quantification [34, 36, 37]. For these reasons, additional methods are required to improve on accuracy and reliability of visual amyloid PET quantification.

In conclusion, this study demonstrates that the visual reading of amyloid PET combined with the deep learning-based estimation of amyloid burden improves the visual interpretation in terms of confidence in the reading and inter-reader agreement. Clinical decisions and management plans depend on the clinical diagnosis of cognitive disorders and those are highly affected by the reading of amyloid PET [38]. Therefore, reliable interpretation of amyloid PET is critical in the diagnosis and further management plan. By reducing disagreement cases particularly for amyloid PET with equivocal amyloid positivity, the deep learning-based amyloid burden estimation system could make the diagnosis more reliable. Furthermore, the one-step estimation method would support visual reading for experts as well as trainees as it can be used in the busy clinical setting.

**Authors' contributions** H.C. designed the study. J.Y.K. performed image analysis. D.Y.L. and K.S. contributed to collect and analyze clinical data. J.Y.K., D.O., and H.C. contributed to the image interpretation. J.Y.K. and D.O. contributed to the data collection and literature review. J.C.P., G.J.C., K.W.K., and D.S.L. contributed to data interpretation and analysis. J.Y.K. and H.C. wrote the manuscript mainly and all authors critically reviewed the manuscript.

**Funding** This research was financially supported by the National Research Foundation of Korea Grant funded by the Korea Government (No. NRF-2019K1A3A1A14065446 and NRF-2019R1F1A1061412).

**Data availability** Data that support this study can be made available upon reasonable request.

## Compliance with ethical standards

**Competing interests** The authors declare that they have no competing interests.

**Ethics approval and consent to participate** All procedures performed in studies involving human participants were following the ethical standards of the institutional and/or national research committee and with the 1964 Helsinki declaration and its later amendments or comparable ethical standards. Informed consent to clinical testing and neuroimaging approved by the institutional review boards of participating institutions (SNUH IRB Registration Number 2004-047-1116).

**Consent for publication** Not applicable.

## References

- 2020 Alzheimer's disease facts and figures. *Alzheimers Dement*. 2020. doi:<https://doi.org/10.1002/alz.12068>.
- Bacsikai BJ, Kajdasz ST, Christie RH, Carter C, Games D, Seubert P, et al. Imaging of amyloid-beta deposits in brains of living mice permits direct observation of clearance of plaques with immunotherapy. *Nat Med*. 2001;7:369–72. <https://doi.org/10.1038/85525>.
- Morris JC, Roe CM, Xiong C, Fagan AM, Goate AM, Holtzman DM, et al. APOE predicts amyloid-beta but not tau Alzheimer pathology in cognitively normal aging. *Ann Neurol*. 2010;67:122–31. <https://doi.org/10.1002/ana.21843>.
- Jack CR Jr, Barrio JR, Kepe V. Cerebral amyloid PET imaging in Alzheimer's disease. *Acta Neuropathol*. 2013;126:643–57. <https://doi.org/10.1007/s00401-013-1185-7>.
- Dementia key facts. WHO. 21. MAR ed; 2019.
- Clark CM, Schneider JA, Bedell BJ, Beach TG, Bilker WB, Mintun MA, et al. Use of florbetapir-PET for imaging beta-amyloid pathology. *Jama-J Am Med Assoc*. 2011;305:275–83. <https://doi.org/10.1001/jama.2010.2008>.
- Minoshima S, Drzezga AE, Barthel H, Bohnen N, Djekidel M, Lewis DH, et al. SNMMI procedure standard/EANM practice guideline for amyloid PET imaging of the brain 1.0. *J Nucl Med*. 2016;57:1316–22. <https://doi.org/10.2967/jnumed.116.174615>.
- Nayate AP, Dubroff JG, Schmitt JE, Nasrallah I, Kishore R, Mankoff D, et al. Use of standardized uptake value ratios decreases interreader variability of [F-18]florbetapir PET brain scan interpretation. *Am J Neuroradiol*. 2015;36:1237–44. <https://doi.org/10.3174/ajnr.A4281>.
- Pontecorvo MJ, Arora AK, Devine M, Lu M, Galante N, Siderowf A, et al. Quantitation of PET signal as an adjunct to visual interpretation of florbetapir imaging. *Eur J Nucl Med Mol I*. 2017;44:825–37. <https://doi.org/10.1007/s00259-016-3601-4>.
- Alongi P, Sardina DS, Coppola R, Scalisi S, Puglisi V, Arnone A, et al. 18F-Florbetaben PET/CT to assess Alzheimer's disease: a new analysis method for regional amyloid quantification. *J Neuroimaging*. 2019;29:383–93. <https://doi.org/10.1111/jon.12601>.
- Bourgeat P, Villemagne VL, Dore V, Brown B, Macaulay SL, Martins R, et al. Comparison of MR-less PiB SUVR quantification methods. *Neurobiol Aging*. 2015;36(Suppl 1):S159–66. <https://doi.org/10.1016/j.neurobiolaging.2014.04.033>.
- Bourgeat P, Dore V, Fripp J, Villemagne V, Rowe C, Salvado O. Computational analysis of PET by AIBL (CapAIBL): a cloud-based processing pipeline for the quantification of PET images. *J Nucl Med*. 2015;56.
- Zhou L, Salvado O, Dore V, Bourgeat P, Raniga P, Macaulay SL, et al. MR-less surface-based amyloid assessment based on 11C PiB PET. *PLoS One*. 2014;9:e84777. <https://doi.org/10.1371/journal.pone.0084777>.
- Kim JY, Suh HY, Ryoo HG, Oh D, Choi H, Paeng JC, et al. Amyloid PET quantification via end-to-end training of a deep learning. *Nucl Med Molec Imag*. 2019;53:340–8. <https://doi.org/10.1007/s13139-019-00610-0>.
- Kim JP, Kim J, Kim Y, Moon SH, Park YH, Yoo S, et al. Staging and quantification of florbetaben PET images using machine learning: impact of predicted regional cortical tracer uptake and amyloid stage on clinical outcomes. *Eur J Nucl Med Mol Imaging*. 2020;47:1971–83. <https://doi.org/10.1007/s00259-019-04663-3>.
- American Psychiatric Association., American Psychiatric Association. Task Force on DSM-IV. Diagnostic and statistical manual of mental disorders : DSM-IV. 4th ed. Washington, DC: American Psychiatric Association; 1994.
- Mckhann G, Drachman D, Folstein M, Katzman R, Price D, Stadlan EM. Clinical-diagnosis of Alzheimers-disease - report of the Nincds-Adrda Work Group under the Auspices of Department-of-Health-and-Human-Services Task-Force on Alzheimers-Disease. *Neurology*. 1984;34:939–44. <https://doi.org/10.1212/Wnl.34.7.939>.

18. Roman GC, Tatemichi TK, Erkinjuntti T, Cummings JL, Masdeu JC, Garcia JH, et al. Vascular dementia - diagnostic-criteria for research studies - report of the Ninds-Airen International Workshop. *Neurology*. 1993;43):250–60. <https://doi.org/10.1212/Wnl.43.2.250>.
19. McKeith IG, Dickson DW, Lowe J, Emre M, O'Brien JT, Feldman H, et al. Diagnosis and management of dementia with Lewy bodies - third report of the DLB consortium. *Neurology*. 2005;65:1863–72. <https://doi.org/10.1212/01.wnl.0000187889.17253.b1>.
20. Neary D, Snowden JS, Gustafson L, Passant U, Stuss D, Black S, et al. Frontotemporal lobar degeneration: a consensus on clinical diagnostic criteria. *Neurology*. 1998;51:1546–54. <https://doi.org/10.1212/wnl.51.6.1546>.
21. Winblad B, Palmer K, Kivipelto M, Jelic V, Fratiglioni L, Wahlund LO, et al. Mild cognitive impairment—beyond controversies, towards a consensus: report of the International Working Group on Mild Cognitive Impairment. *J Intern Med*. 2004;256:240–6. <https://doi.org/10.1111/j.1365-2796.2004.01380.x>.
22. Jansen WJ, Ossenkoppele R, Knol DL, Tijms BM, Scheltens P, Verhey FRJ, et al. Prevalence of cerebral amyloid pathology in persons without dementia a meta-analysis. *Jama-J Am Med Assoc*. 2015;313:1924–38. <https://doi.org/10.1001/jama.2015.4668>.
23. Sabri O, Seibyl J, Rowe C, Barthel H. Beta-amyloid imaging with florbetaben. *Clin Transl Imaging*. 2015;3:13–26. <https://doi.org/10.1007/s40336-015-0102-6>.
24. Landau SM, Fero A, Baker SL, Koeppe R, Mintun M, Chen K, et al. Measurement of longitudinal beta-amyloid change with 18F-florbetapir PET and standardized uptake value ratios. *J Nucl Med*. 2015;56:567–74. <https://doi.org/10.2967/jnumed.114.148981>.
25. Payoux P, Delrieu J, Gallini A, Adel D, Salabert AS, Hitzel A, et al. Cognitive and functional patterns of nondemented subjects with equivocal visual amyloid PET findings. *Eur J Nucl Med Mol Imaging*. 2015;42:1459–68. <https://doi.org/10.1007/s00259-015-3067-9>.
26. Barthel H, Sabri O. Clinical use and utility of amyloid imaging. *J Nucl Med*. 2017;58:1711–7. <https://doi.org/10.2967/jnumed.116.185017>.
27. Oh M, Seo M, Oh SY, Kim H, Choi BW, Oh JS, et al. Clinical significance of visually equivocal amyloid PET findings from the Alzheimer's Disease Neuroimaging Initiative cohort. *Neuroreport*. 2018;29:553–8. <https://doi.org/10.1097/Wnr.0000000000000986>.
28. Okada Y, Kato T, Iwata K, Kimura Y, Nakamura A, Hattori H, et al. Evaluation of PiB visual interpretation with CSF A beta and longitudinal SUVR in J-ADNI study. *Ann Nucl Med*. 2020;34:108–18. <https://doi.org/10.1007/s12149-019-01420-2>.
29. Yamane T, Ishii K, Sakata M, Ikari Y, Nishio T, Ishii K, et al. Inter-rater variability of visual interpretation and comparison with quantitative evaluation of (11)C-PiB PET amyloid images of the Japanese Alzheimer's Disease Neuroimaging Initiative (J-ADNI) multicenter study. *Eur J Nucl Med Mol Imaging*. 2017;44:850–7. <https://doi.org/10.1007/s00259-016-3591-2>.
30. Harn NR, Hunt SL, Hill J, Vidoni E, Perry M, Burns JM. Augmenting amyloid PET interpretations with quantitative information improves consistency of early amyloid detection. *Clin Nucl Med*. 2017;42:577–81. <https://doi.org/10.1097/RLU.0000000000001693>.
31. Cho SH, Choe YS, Kim HJ, Jang H, Kim Y, Kim SE, et al. A new Centiloid method for (18)F-florbetaben and (18)F-flutemetamol PET without conversion to PiB. *Eur J Nucl Med Mol Imaging*. 2020;47:1938–48. <https://doi.org/10.1007/s00259-019-04596-x>.
32. Klunk WE, Koeppe RA, Price JC, Benzinger TL, Devous MD Sr, Jagust WJ, et al. The Centiloid Project: standardizing quantitative amyloid plaque estimation by PET. *Alzheimers Dement*. 2015;11:1–15 e1–4. <https://doi.org/10.1016/j.jalz.2014.07.003>.
33. Becker JA, Hedden T, Carmasin J, Maye J, Rentz DM, Putcha D, et al. Amyloid-beta associated cortical thinning in clinically normal elderly. *Ann Neurol*. 2011;69:1032–42. <https://doi.org/10.1002/ana.22333>.
34. Ripolles P, Marco-Pallares J, de Diego-Balaguer R, Miro J, Falip M, Juncadella M, et al. Analysis of automated methods for spatial normalization of lesioned brains. *Neuroimage*. 2012;60:1296–306. <https://doi.org/10.1016/j.neuroimage.2012.01.094>.
35. Reig S, Penedo M, Gispert JD, Pascau J, Sanchez-Gonzalez J, Garcia-Barreno P, et al. Impact of ventricular enlargement on the measurement of metabolic activity in spatially normalized PET. *Neuroimage*. 2007;35:748–58. <https://doi.org/10.1016/j.neuroimage.2006.12.015>.
36. van Westen D, Lindqvist D, Blennow K, Minthon L, Nagga K, Stomrud E, et al. Cerebral white matter lesions - associations with A beta isoforms and amyloid PET. *Sci Rep*. 2016;6:20709. <https://doi.org/10.1038/srep20709>.
37. Johnson VE, Stewart W, Smith DH. Traumatic brain injury and amyloid-beta pathology: a link to Alzheimer's disease? *Nat Rev Neurosci*. 2010;11:361–70. <https://doi.org/10.1038/nrn2808>.
38. Rabinovici GD, Gatsonis C, Apgar C, Chaudhary K, Gareen I, Hanna L, et al. Association of amyloid positron emission tomography with subsequent change in clinical management among Medicare beneficiaries with mild cognitive impairment or dementia. *Jama-J Am Med Assoc*. 2019;321:1286–94. <https://doi.org/10.1001/jama.2019.2000>.

**Publisher's note** Springer Nature remains neutral with regard to jurisdictional claims in published maps and institutional affiliations.